

---

For correspondence  
gsk20@cam.ac.uk (GSKS);  
della.david@dzne.de (DCD)

---

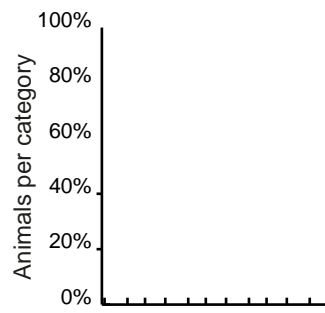


## su ts

JA p n nt f tn prot ns r ntr ns pron to  
t n rt nt ssu s

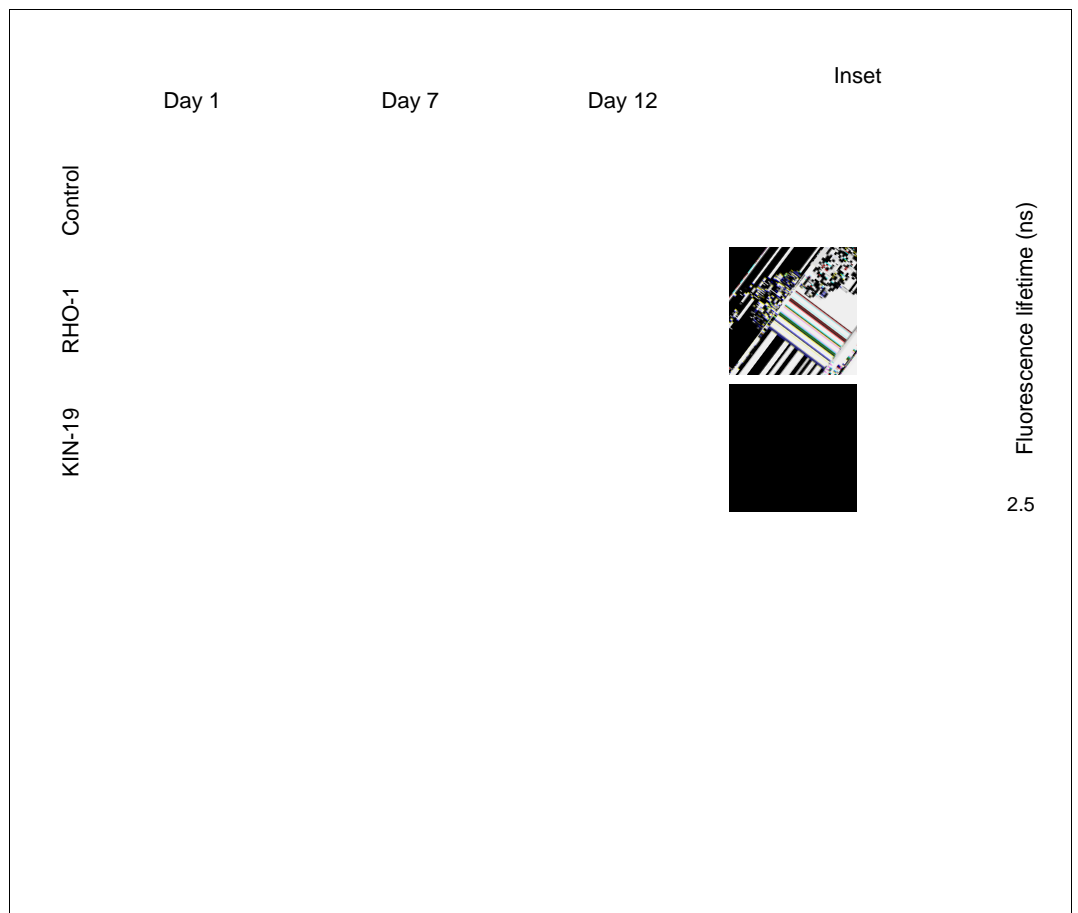
Previously, we performed an extensive characterization of the aggregation of two proteins, casein kinase I isoform alpha (KIN-19) and Ras-like GTP-binding protein rhoA (RHO-1). Both KIN-19 and RHO-1 were identified among the proteins with the highest propensity to become insoluble with age in wild-type *C. elegans* somatic tissues (David *et al.*, 2010). In vivo analysis of animals expressing these proteins fused to fluorescent tags showed the appearance of immobile deposits with age (David *et al.*, 2010). Among the insoluble proteome, the enrichment of certain physico-chemical features such as high aliphatic amino acid content or propensity to form  $\beta$ -sheet-rich structures shows that age-dependent protein aggregation is not random (David *et al.*, 2010; Lechler *et al.*, 2017; Walther *et al.*, 2015). To understand whether KIN-19 and RHO-1 have an intrinsic capacity to aggregate similar to disease-associated proteins or whether a progressive accumulation of protein damage caused by non-enzymatic posttranslational modifications is required to induce their aggregation, we evaluated the dynamics of protein aggregation in vivo. Protein labeling with mEOS2, a green-to-red photoconvertible fluorescent protein, has been successfully used to track protein dynamics (McKinney *et al.*, 2009). In the present case, we used the mEOS2 tag to investigate how fast newly synthesized KIN-19 and RHO-1 aggregate. For this purpose, we generated transgenic animals expressing KIN-19::mEOS2 in either the pharynx or in the body-wall muscles and transgenic animals expressing RHO-1::mEOS2 in the pharynx. The mEOS2 tag did not disrupt the aggregation potential of KIN-19, as the absence of fluorescence recovery after photobleaching confirms that both KIN-19::mEOS2 puncta in the pharynx and body-wall muscle are highly immobile structures (

**B**



Aggregation level  
(green emitting):

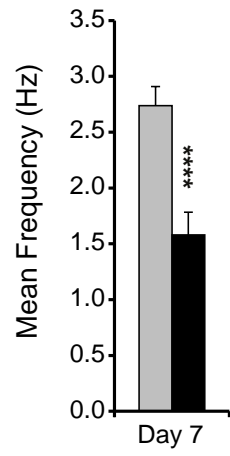
fluorescent-tagged amyloid proteins due to quenching (*Chen et al., 2017; Kaminski Schierle et al., 2011; Murakami et al., 2015*). In the current study, we applied FLIM to determine whether KIN-19 and RHO-1 form amyloid-like aggregates in live *C. elegans*. For this, we generated transgenic animals expressing translational fusions with the yellow fluorescent protein Venus in the pharynx. We





**A** Pumping  
Pharyngeal KIN-19::tagRFP

Thrashing  
Body-wall muscle KIN-19::tagRFP



Aggregation level:  
□ Low ■ High

Aggregation level:  
□ Low ■ High

**C**

Thrashing  
Body-wall muscle RHO-1::Venus  
(no aggregation)





## **D s u s s o n**

**Widespread protein aggregation in the context of normal aging has been observed in *C. elegans* (David et al., 2010; Reis-Rodrigues et al., 2012; Walther et al., 2015), *Drosophila* (Demontis and Perrimon, 2010), *Saccharomyces cerevisiae* (Peters et al., 2012**

**Our findings predict that age-dependent protein aggregation would result from decreased levels of molecular chaperones linked to protein synthesis rather than molecular chaperones induced by stress (Albanèse *et al.*, 2006; Pechmann *et al.*, 2013). Impaired proteasome-mediated removal of unfolded proteins directly after synthesis (Schubert *et al.*, 2000) could also significantly contribute**



Source	Designation	Manufacturer	Concentration
Chemical compound, drug	X34	SML1954, Sigma-Aldrich, Germany	1 mM final
Chemical compound, drug	thioflavin T	#ab120751, abcam, UK	50 $\mu$ M
Commercial assay or kit	5-Hydroxytryptamine creatinine sulfate complex	H7752, Sigma-Aldrich, Germany	10 $\mu$ M
Commercial assay or kit	Nickel Sepharose 6 Fast Flow beads from HisTrap FF Crude column	GE Healthcare, Uppsala, Sweden	

## Construction

Cloning was carried out using the Gateway system (Life Technologies, Darmstadt, Germany). *Pmyo-2* promoter and pKA1062 mEOS2 translational vector were kindly provided by Dr. Brian Lee and Dr. Kaveh Ashrafi, UCSF. *rho-1* cDNA was amplified from a cDNA library prepared from total RNA isolated from N2 worms. Plasmid containing biotinylation enzyme birA was kindly provided by Dr. Ekkehard Schulze (University Freiburg). All constructs contain the *unc-54* 3' UTR. The *tagRFP* vector was obtained from Evrogen (AXXORA, San Diego, CA). Venus was generated by targeted mutation of the *yfp* gene. HisAvi-tagged KIN-19 and RHO-1 were generated by cloning at the C-terminus a RGS6 tag together with a bacterially derived polypeptide serving as a biotinylation signal in vivo as previously described (Schäffer *et al.*, 2010; Tagwerker *et al.*, 2006). Constructs were sequenced at each step. Transgenics were generated by microinjection of the constructs at concentrations between 10 and 50 ng/ $\mu$ l into N2 animals. Stable lines were generated by irradiating the animals containing the extrachromosomal array in a CL-1000 Ultraviolet Crosslinker (UVP) with 275  $\mu$ J x 100. 100% transmission lines were backcrossed at least four times into the wild-type N2 strain.

## Intention

All strains were kept at 15°C on NGM plates inoculated with OP50 using standard techniques. Age-synchronization was achieved by transferring adults of the desired strain to 20°C and selecting their progeny at L4 stage. All experiments were performed at 20°C. Day 1 of adulthood starts 24 hr after L4.

## Photoconversion of Venus

For photoconversion, worms were transferred onto a small (diameter 35 mm) NGM plate without food. The plate was placed 0.5 cm below a collimator (Collimator High-End Lumencor, Leica, Germany) fitted with a filter for blue fluorescence (387/11 BrightLine HC, diameter 40 mm) and illuminated by a Lumencor Sola SE II (AHF, Tübingen). Conversion of mEOS2 in transgenic animals was performed four times for five minutes, with 2 min pauses between exposures. To reduce translation, worms were placed 2 hr before conversion on bacterial seeded plates with 500  $\mu$ g/ml cycloheximide and kept after conversion on plates with cycloheximide for 48 hr during aggregation quantification.

## Aggregation quantification in vivo

Aggregation levels were determined using Leica fluorescence microscope M165 FC with a Planapo 2.0x objective. Aggregation was quantified following pre-set criteria adapted to the transgene expression pattern and levels in the different transgenic *C. elegans* models: Animals expressing *Pkin-19::KIN-19::mEOS2*, *Pkin-19::KIN-19::Venus* or *Pkin-19::KIN-19::TagRFP* were divided into less than 10 puncta (low aggregation), between 10 and 100 puncta (medium aggregation) and over 100 puncta in the anterior pharyngeal bulb (high aggregation). Animals overexpressing *Pmyo-2::RHO-1::Venus* were divided into less than 10 puncta in anterior or posterior pharyngeal bulb (low aggregation), over 10 puncta in either bulbs (medium aggregation) and over 10 puncta in both bulbs (high aggregation). Because of extensive RHO-1 aggregation in animals overexpressing *Pmyo-2::RHO-1::*



## XL st rñ

Worms were incubated in 1 mM X-34 in 10 mM Tris-HCl pH 8 for 2 hr, gently shaking at room temperature as previously described (*Link et al., 2001*). Worms were then transferred to bacteria seeded NGM plates to destain overnight before confocal imaging.

## rñ pu rñ n s s

Electrical activity of the pharyngeal pumping was measured using the NemaMetrix ScreenChip System (NemaMetrix, Eugene, OR). The entire setup is housed in a laboratory that maintained a temperature of approximately 21°C. Baseline noise was typically between 5 and 25  $\mu$ V.

For each experiment, 50 worms were picked in 1.5 ml of M9 +0.01% Triton and washed three times via low-speed centrifugation. Worms were resuspended in 1.5 ml M9 +0.01% Triton + 10  $\mu$ M 5-Hydroxytryptamine creatinine sulfate complex (Serotonin creatinine sulfate monohydrate) (Sigma, H7752) and incubated for 20 min. The ScreenChip system was placed on a stereoscope and loaded with a fresh screen chip. The screen chip was then vacuum-filled with M9 +0.01% Triton+10  $\mu$ M 5-Hydroxytryptamine creatinine sulfate complex and the NemaAcquire software initiated for baseline noise checking. The animals were loaded into the recording channel of the screen chip via vacuum. After loading each animal, we waited at least 30 s or until the pumping became regular before starting to record. Each animal was recorded for approximately 2 min regardless of whether pumping activity was observed or not. Between 20 and 40 animals were recorded for each condition.

The recordings were analyzed by NemaAnalysis v0.2 software using the 'Brute Force' optimization method. The ideal settings were chosen automatically from all combinations of the bounds settings (Minimum SNR from 1.4 (low) to 2.0 (high), with a Step size of 0.1; Highpass Cutoff from 10 (low) to 20 (high), with a Step size of 5) and applied to produce the analysis results. Data was exported into Excel for statistical analysis with the student's t test.

## r s rñ n s s

To quantify movement in terms of body-bends-per-second, movies of worms swimming in liquid were acquired with high frame rates (15 frames per second) using a high-resolution monochrome camera (JAI BM-500 GE, Stemmer imaging GmbH, Puchheim, Germany). For each condition, around 40 animals were filmed (see *Supplementary file 1* for exact numbers). Worms were picked from cultivation plate and allowed to swim in a small plastic petri dish filled with M9 +0.01% Triton. Petri

**significantly thinner or highly wrinkled, or with large empty space between. The pharyngeal muscle structure was considered severely defective when the actin filament structure showed large holes.**

stabilizing buffer and 1 ml of the protein loaded onto the columns by injection. Cleaved RHO-1 was eluted in stabilization buffer during the column wash. The fusion tag and the His-tagged TEV were





acquisition; Gabriele S Kaminski Schierle, Conceptualization, Resources, Supervision, Funding acquisition, Writing—original draft, Project administration, Writing—review and editing; Della C David, Conceptualization, Resources, Formal analysis, Supervision, Funding acquisition, Validation, Investigation, Visualization, Methodology, Writing—original draft, Project administration, Writing—review and editing

[Author ORCIDs](#)

**Amberley D Stephens**

---

---



- nn n , Mendell JR, Kuret J. 2008. Casein kinase 1 alpha associates with the tau-bearing lesions of inclusion body myositis. *Neuroscience Letters* 437:141–145. DOI: <https://doi.org/10.1016/j.neulet.2007.11.066>, PMID: 18191026
- r l, Frumkin A, Dror S, Shemesh N, Shai N, Ben-Zvi A. 2013. Using *Caenorhabditis elegans* as a model system to study protein homeostasis in a multicellular organism. *Journal of Visualized Experiments* 8:e50840. DOI: <https://doi.org/10.3791/50840>
- rn A, Ackermann B, Clement AM, Duerk H, Behl C. 2010. HSF1-controlled and age-associated chaperone capacity in neurons and muscle cells of *C. elegans*. *PLOS ONE* 5:e8568. DOI: <https://doi.org/10.1371/journal.pone.0008568>, PMID: 20052290
- rst n , Morito D, Kakahana T, Sugihara M, Minnen A, Hipp MS, Nussbaum-Krammer C, Kasturi P, Hartl FU, Nagata K, Morimoto RL. 2015. Proteotoxic stress and ageing triggers the loss of redox homeostasis across cellular compartments. *The EMBO Journal* 34:2334–2349. DOI: <https://doi.org/10.15252/embj.201591711>, PMID: 26228940
- no s , Vendruscolo M, Dobson CM. 2014. The amyloid state and its association with protein misfolding diseases. *Nature Reviews Molecular Cell Biology* 15:384–396. DOI: <https://doi.org/10.1038/nrm3810>, PMID: 24854788
- ur t , Johnson GS, Cha D, Christenson ER, DeMaggio AJ, Hoekstra MF. 1997. Casein kinase 1 is tightly associated with paired-helical filaments isolated from Alzheimer's disease brain. *Journal of Neurochemistry* 69:2506–2515. DOI: <https://doi.org/10.1046/j.1471-4159.1997.69062506.x>, PMID: 9375684
- ut ns پت ر , Stephens AD, Fusco G, Ströhl F, Curry N, Zacharopoulou M, Michel CH, Laine R, Nespovitaya N, Fantham M, Pinotsi D, Zago W, Fraser P, Tandon A, St George-Hyslop P, Rees E, Phillips JJ, De Simone A,

ts , Rardin MJ, Czerwieniec G, Evani US, Reis-Rodrigues P, Lithgow GJ, Mooney SD, Gibson BW, Hughes RE. 2012. Tor1 regulates protein solubility in *Saccharomyces cerevisiae*. *Molecular Biology of the Cell* 1:4679-

Yu A